Scintillation Spectra of Scattered Electromagnetic Waves in Turbulent Magnetized Plasma

George Jandieri[*1], Zhuzhuna Diasamidze[2], Mzia Diasamidze[3]

[1]Physics Department, Georgian Technical University, 77 Kostava Str. 0175, Tbilisi, Georgia

[2]Batumi Shota Rustaveli State University, 35 Ninoshvili Str., 6010 Batumi, Georgia

[3]Batumi State Maritime Academy, 53 Rustaveli Av., 6010 Batumi, Georgia

[*1]jandieri@access.sanet.ge; [2]zhuzhuna.diasamidze@gmail.com; [3]mzia.diasamidze@gmail.com

***Abstract*- Second order statistical moments of scattered ordinary and extraordinary waves in magnetized turbulent plasma are investigated analytically and numerically using the smooth perturbation method. Correlation functions of the phase fluctuations are obtained in the principle and perpendicular planes for arbitrary correlation functions of electron density fluctuations. New features of both the Double-humped effect and scintillation spectra are analysed for anisotropic Gaussian and power-law wavenumber spectra taking into account diffraction effects. The scintillation level is estimated for different anisotropy factors and the angle of inclination of prolate irregularities with respect to the external magnetic field. Scintillation minimums of a temporal spectrum are calculated for different thicknesses of a plasma slab taking into account the movement of rigid irregularities and diffraction effects for scattered ordinary and extraordinary waves in turbulent magnetized plasma.**

Keywords*- *Statistical Moments; Extraordinary Wave; Fluctuations; Power Spectrum; Radio Wave

I. INTRODUCTION

The fluctuations in amplitude and phase (scintillation) of radio waves passing through the ionosphere are caused by spatial irregularities in the electron density. The sizes of ionospheric irregularities have been obtained by several techniques, including topside sounding, radio-satellite scintillations and direct measurements by satellite probes. The irregularities have a variety of sizes and usually are elongated in the magnetic field direction [1]. The connection between phase and amplitude fluctuations and the irregularities causing them has been studied in [2, 3], where the passage of radiation of optical wavelength through a turbulent atmosphere is discussed for the case when the scattering is weak and the resulting scintillations are small. The presence of geomagnetic field leads to the birefringence and anisotropy. Information about the irregularity velocity, the equivalent thickness of the scattering layer, and the irregularity electron density spectrum can be deduced using conventional diffraction theory. For relatively small irregularities diffraction effects are important.

The features of the spatial power spectrum (SPS) of scattered radiation in magnetized anisotropic plasma in the complex geometrical optics approximation using the perturbation method have been investigated in [4, 5]. The power spectra of scintillation signals can yield valuable information about wavy processes in plasma and the structure of the irregularities. Evolution of the angular distribution of ray intensity at light propagation in random medium with prolate irregularities has been investigated [6] using the smooth perturbation method. It has been shown that the SPS of a multiple scattered radiation at oblique illumination of random medium by mono-directed incident radiation has a double-peaked shape. Numerical simulation has been carried out by Monte-Carlo method [7]. It was shown that a strongly pronounced dip exists in the angular spectrum of a single-scattered radiation along the direction of prolate inhomogeneities caused by permittivity fluctuations. The “Double-humped effect” in turbulent anisotropic magnetized plasma has been discovered recently using the smooth perturbation method and taking into account diffraction effects [8, 9].

The present paper reports second order statistical moments of the SPS, new peculiarities of the “Double-humped effect” and the scintillation spectrum of multiple scattered radio waves in randomly inhomogeneous anisotropic magnetized plasma with electron density fluctuations which are investigated analytically and numerically using the smooth perturbation method. The evaluation of a double-peak shape in the SPS of multiple scattered radio waves is analyzed under oblique illumination of turbulent plasma by mono-directed incident radiation taking into account diffraction effects. The results of the analysis of the power spectrum of ionospheric scintillation data, which is related to fluctuations in the radio refractive index in the ionospheric *F* region (at altitudes 200-400 km) are presented. The influence of anisotropic plasma irregularities parameters on the scintillation spectrum is a novelty of this paper. Fresnel oscillations are interpreted for both Gaussian and power-law wavenumber models if plasma irregularities are moving transversely to the line of the sight path. An analytical formulation and numerical calculations have been carried out for both anisotropic Gaussian and power-law wavenumber models in the principle and perpendicular planes for the *F*-region ionosphere using the experimental data.

II. SECOND ORDER STATISTICAL MOMENTS OF SCATTERED ORDINARY AND EXTRAORDINARY RADIO WAVES IN TURBULENT MAGNETIZED PLASMA

The electric field in magnetized turbulent plasma with anisotropic electron density irregularities satisfies wave equation:

$$\left(\frac{\partial^2}{\partial x_i \, \partial x_j} - \Delta \delta_{ij} - k_0^2 \, \varepsilon_{ij}(\mathbf{r}) \right) \mathbf{E_j}(\mathbf{r}) = 0 \tag{1}$$

The absorption in the layer is negligible for a high frequency incident wave. If the electromagnetic wave is propagating along Z axis and the vector $\boldsymbol{\tau}$ lies in the yoz plane $\boldsymbol{k}_{II}\, z$ - principle plane), the components of the second-rank tensor ε_{ij} of the collisionless magnetized plasma are [10]:

$$\varepsilon_{xx} = 1 - \mathrm{v}(1-u)^{-1}, \; \varepsilon_{yy} = 1 - \mathrm{v}(1 - u \sin^2\alpha)\,(1-u)^{-1}$$

$$\tilde{\varepsilon}_{xy} = -\,\tilde{\varepsilon}_{yx} = \mathrm{v}\sqrt{u}\,\cos\alpha\,(1-u)^{-1}, \tilde{\varepsilon}_{xz} = -\,\tilde{\varepsilon}_{zx} = -\,\mathrm{v}\sqrt{u}\,\sin\alpha\,(1-u)^{-1}$$

$$\varepsilon_{zz} = 1 - \mathrm{v}(1 - u\cos^2\alpha)(1-u)^{-1}$$

where α is the angle between $\mathbf{k_0}$ and $\mathbf{H_0}$ vectors (YZ is the principle plane); $\omega_p(\mathbf{r}) = [4\pi N(\mathbf{r})e^2/m]^{1/2}$ is the plasma frequency, $N(\mathbf{r})$ is the electron density, $u(\mathbf{r}) = (eH_0(\mathbf{r})/m\,c\,\omega)^2$ and $\mathrm{v}(\mathbf{r}) = \omega_p^2(\mathbf{r})/\omega^2$ are the magneto-ionic parameters, $\Omega_H = eH_0/mc$ is the electron gyrofrequency, Δ is the Laplacian, δ_{ij} is the Kronecker symbol. The dielectric permittivity of turbulent magnetized plasma is a random function of the spatial coordinates $\varepsilon_{ij}(\mathbf{r}) = \varepsilon_{ij}^{(0)} + \varepsilon_{ij}^{(1)}(\mathbf{r})$, $|\,\varepsilon_{ij}^{(1)}(\mathbf{r})\,| << 1$. The first term is a regular (unperturbed) component of the dielectric permittivity connected with the ionization distribution in the ionospheric layers at different altitudes; the second term is a fluctuating term of the dielectric permittivity describing electron density fluctuations in the ionosphere, which is the random function of the spatial coordinates: $\mathrm{v}(\mathbf{r}) = \mathrm{v}_0\,[1 + n_1(\mathbf{r})]$. We introduce the wave field as $E_j(\mathbf{r}) = E_{0j}\exp\{\Phi(\mathbf{r})\}$, where $\Phi(\mathbf{r})$ is the complex phase, which is presented as a sum $\Phi(\mathbf{r}) = \varphi_0 + \varphi_1 + \varphi_2 + \ldots$, $\varphi_0 = i\,k_0\,x + i\,k_\perp\,y$ ($k_\perp << k_0$). Complex phase fluctuations are of the order $\varphi_1 \sim \varepsilon_{ij}^{(1)}$, $\varphi_2 \sim \varepsilon_{ij}^{(1)\,2}$. The parameter $\mu = k_\perp / k_0$ describing diffraction effects is calculated in the zero-order approximation [9].

Taking into account inequalities characterizing the smooth perturbation method [2, 3]:

$$\left|\frac{\partial\varphi_1}{\partial z}\right| << k_0\,|\,\varphi_1\,|, \quad \left|\frac{\partial^2\varphi_1}{\partial z^2}\right| << k_0\left|\frac{\partial\varphi_1}{\partial z}\right|, \quad \left|\frac{\partial\varphi_2}{\partial z}\right| << k_0\,|\,\varphi_2\,|, \quad \left|\frac{\partial^2\varphi_2}{\partial z^2}\right| << k_0\left|\frac{\partial\varphi_2}{\partial z}\right|,$$

in the first approximation we obtain:

$$\left[\frac{\partial^2\varphi_1}{\partial x_i\,\partial x_j} + \frac{\partial\varphi_0}{\partial x_i}\,\frac{\partial\varphi_1}{\partial x_j} + \frac{\partial\varphi_1}{\partial x_i}\,\frac{\partial\varphi_0}{\partial x_j} - \delta_{ij}\left(\Delta_\perp + 2\,i\,k_\perp\,\frac{\partial\varphi_1}{\partial y} + 2\,i\,k_0\,\frac{\partial\varphi_1}{\partial z} \right) - k_0^2\,\varepsilon_{ij}^{(0)} \right] E_{0j} = 0 \tag{2}$$

where $\Delta_\perp = (\partial^2\varphi_1/\partial x^2) + (\partial^2\varphi_1/\partial y^2)$ is the transversal Laplasian.

Fourier transformation for the phase fluctuations is:

$$\varphi_1(x,y,z) = \int_{-\infty}^{\infty} d\,k_x \int_{-\infty}^{\infty} d\,k_y\;\; \psi(k_x,k_y,z)\,\exp(i\,k_x x + i\,k_y y)\,.$$

The two-dimensional spectral function of the phase fluctuation in the principle plane satisfies the stochastic differential equation [8]:

$$\frac{\partial\psi}{\partial z} + \frac{i}{k_x + i\,\mathrm{P}_j(k_y + k_\perp)}\left[k_0\,k_x + i\,\mathrm{P}_j k_0\,k_y - i\,\Gamma_j(k_x^2 + k_y^2 + 2\,k_\perp\,k_y) \right]\psi = \frac{k_0^2}{k_x + i\,\mathrm{P}_j(k_y + k_\perp)}\,(\tilde{\varepsilon}_{xz}^{(1)} + \varepsilon_{yz}^{(1)}\,\mathrm{P}_j + \varepsilon_{zz}^{(1)}\,\Gamma_j) \tag{3}$$

The presence of the geomagnetic field leads to the birefringence and anisotropy. Polarization coefficients are [10]:

$$\mathrm{P}_j = \frac{2\sqrt{u}\,(1-\mathrm{v})\cos\alpha}{u\sin^2\alpha \pm \sqrt{u^2\sin^4\alpha + 4u(1-\mathrm{v})^2\cos^2\alpha}}, \qquad \Gamma_j = -\frac{\mathrm{v}\sqrt{u}\sin\alpha + \mathrm{P}_j\,u\,\mathrm{v}\sin\alpha\cos\alpha}{1 - u - \mathrm{v} + u\,\mathrm{v}\cos^2\alpha},$$

the upper sign (index $j = 1$) corresponds to the extraordinary wave (*e*-wave) and the lower sign (index $j = 2$) - to the ordinary wave (*o*-wave). These waves in magnetized plasma generally are elliptically polarized. The external magnetic field radically changes electromagnetic properties of plasma making it a magnetized (gyrotropic and anisotropic) medium. Gyrotropy of plasma is revealed in elliptic polarization of normal waves; anisotropy appears in the direction of propagation depending on wave characteristics (polarization, refractive index and absorption).

The solution of Equation (3) with the boundary condition $\psi(k_x,\, k_y,\, z=0)=0$ is (see also [8]):

$$\psi(k_x,k_y,L)=\frac{k_0^2\left[k_x-i\,\mathrm{P}_j(k_y+k_\perp)\right]}{\Phi_3}\int_0^L dz'\left[\tilde{\varepsilon}_{xz}^{(1)}(k_x,k_y,z')+\mathrm{P}_j\,\tilde{\varepsilon}_{yz}^{(1)}(k_x,k_y,z')+\Gamma_j\,\tilde{\varepsilon}_{zz}^{(1)}(k_x,k_y,z')\right]\cdot$$
$$\cdot\exp\left[-\frac{\Phi_1+i\,\Phi_2}{\Phi_3}\,k_0\,(L-z')\right] \tag{4}$$

where

$$\Phi_1=\delta_1\,x+\Gamma_j\,x^3,\;\delta_1=\mathrm{P}_j\,\mu+\Gamma_j\,s(2\,\mu+s),\;\Phi_2=\delta_2\,x^2+\delta_3,\;\delta_2=1-\mathrm{P}_j\,\Gamma_j\,(\mu+s)$$

$$\Phi_3=x^2+\delta_4\,,\;\delta_4=\mathrm{P}_j^2\,(\mu+s)^2\,,\;\delta_3=\mathrm{P}_j\,s\left[\mathrm{P}_j(\mu+s)-\Gamma_j(2\mu^2+3\mu s+s^2)\right],\;x=k_x/k_0\,,\;s=k_y/k_0\,.$$

We can calculate second order statistical moments of scattered electromagnetic waves in a randomly inhomogeneous magnetized plasma using Equation (4), changing the variables $z'-z''=\rho_z$, $z'+z''=2\eta$ using the relationship $<\mathrm{T}_{\alpha\beta}(\boldsymbol{\kappa},z')\;\mathrm{T}_{\gamma\delta}^{*}(\boldsymbol{\kappa}',z'')>=W_{\alpha\beta,\gamma\delta}(\boldsymbol{\kappa},z'-z'')\;\delta(\boldsymbol{\kappa}-\boldsymbol{\kappa}')$, where $W_{\alpha\beta,\gamma\delta}(\boldsymbol{\kappa},z'-z'')$ is the 2D spatial spectrum of electron density fluctuations, the indices denote the product of fluctuating components of the second rank tensor describing magnetized plasma, δ is Dirac delta function, k_x and k_y are the spatial wavenumber components in the directions *x* and *y*, respectively, *L* is the propagation distance.

Using (4) and taking into account the well-known expression [2, 3]: $<\varepsilon_{\alpha\beta}(\boldsymbol{\kappa},z')\;\varepsilon_{\gamma\delta}^{*}(\boldsymbol{\kappa}',z'')>=V_{\alpha\beta,\gamma\delta}(\boldsymbol{\kappa},z'-z'')\,\delta(\boldsymbol{\kappa}-\boldsymbol{\kappa}')$, changing the variables $z'-z''=\rho_z$, $z'+z''=2\eta$ and following calculations [8] we obtain the second order statistical moments of scattered electromagnetic waves for arbitrary correlation functions of electron density. Correlation functions of the phase fluctuations of scattered ordinary and extraordinary radio waves for the arbitrary correlation function of electron density fluctuations in the principle and perpendicular planes are:

$$W_\varphi^{(\parallel)}(\xi,\,\eta,L)\;=\;\tilde{\Omega}_2\int_{-\infty}^{\infty}ds\int_{-\infty}^{\infty}dx\;\frac{x^2+\mathrm{P}_j^2\,(\mu+s)^2}{(\delta_4+x^2)^2}\;V_N\left(x,\;s,-\frac{\Phi_2}{\Phi_3}\right)\exp(-\,i\,\xi\,x-i\,\eta\,s)\,, \tag{5}$$

$$W_\varphi^{(\perp)}(\xi,\,\eta,L)\;=\frac{\pi}{2}\,k_0^4\,L\,\Omega_1\int_{-\infty}^{\infty}ds\int_{-\infty}^{\infty}dx\;V_N\left[x,\;s,\;-\frac{1}{4}(x^2\,d_1+d_2)\right]\exp(-\,i\,\xi\,x-i\,\eta\,s)\,, \tag{6}$$

where

$$\Omega_2=\frac{\mathrm{v}_0^2\,u_0}{(1-u_0)^2}\,(\sin^2\alpha+2\,\mathrm{P}_j\,\sqrt{u_0}\,\sin^2\alpha\,\cos\alpha-2\,\Gamma_j\,\sqrt{u_0}\,\sin\alpha\,\cos^2\alpha-2\,\mathrm{P}_j\,\Gamma_j\,u_0\,\sin\alpha\,\cos^3\alpha+\mathrm{P}_j^2\,u_0\,\sin^2\alpha\,\cos^2\alpha$$

$$+\,\Gamma_j^2\,u_0\,\cos^4\alpha)\,,\;\Omega_1=\frac{\mathrm{v}_0^2}{(1-u_0)^2}\left[1+u_0-2\,\sqrt{u_0}\,(\sin\alpha-\cos\alpha+\sqrt{u_0}\,\sin\alpha\cos\alpha)\right],\;\tilde{\Omega}_2=B_0\,\Omega_2\,T^2/\pi\,\chi\,,\;\eta=k_0\,\rho_y\,,$$

$$\xi=k_0\,\rho_x\,,\;B_0=\sigma_n^2\,\sqrt{\pi}\,T\,k_0\,L/4\,\chi\,,\;d_2=2\,s\,(s+2\,\mu)\,,\;d_1=\Gamma_j\left[\mathrm{P}_j\,(s+\mu)+\Gamma_j\right]$$

ρ_y and ρ_x are distances between observation points spaced apart in the principle and perpendicular planes, respectively. From Equation (6) follows that in non-magnetized plasma $H_0=0$ at $\chi=1$ (isotropic case), neglecting diffraction effects ($\mu=0$), the power spectrum of the phase fluctuations $W_\varphi(k_x,k_y,L)$ and the power spectrum of the electron density fluctuations $V_N(k_x,k_y,k_z)$ are related to the well-known formula [3] $W_\varphi(k_x,k_y,L)=2\,\pi(r_e\,\lambda)^2\,L\,V_N(k_x,k_y,k_z=0)$, where r_e is the classical electron radius.

The wave structure functions [1, 2]:

$$D_1(\mathbf{r}_1,\mathbf{r}_2) = <\left(\varphi_1(\mathbf{r}_1)-\varphi_1(\mathbf{r}_2)\right)\left(\varphi_1^*(\mathbf{r}_1)-\varphi_1^*(\mathbf{r}_2)\right)>,\quad D_2(\mathbf{r}_1,\mathbf{r}_2) = <\left(\varphi_1(\mathbf{r}_1)-\varphi_1(\mathbf{r}_2)\right)^2>, \tag{7}$$

of the amplitude, phase and mutual correlation functions:

$$D_\chi(\mathbf{r}_1,\mathbf{r}_2) = \frac{1}{2}(D_1 + \mathrm{Re}\,D_2),\quad D_S(\mathbf{r}_1,\mathbf{r}_2) = \frac{1}{2}(D_1 - \mathrm{Re}\,D_2),\quad D_{\chi S} = \frac{1}{2}\,\mathrm{Im}\,D_2. \tag{8}$$

are functions of the separation distance $\rho_{x,y}$, the propagation distance L, and the plasma parameters.

The transverse correlation function of a scattered field $W_{EE^*}(\boldsymbol{\rho}) = <E(\mathbf{r})\,E^*(\mathbf{r}+\boldsymbol{\rho})>$ is expressed via the correlation function and the variance of the phase fluctuations [4, 7, 8]:

$$W_{EE^*}(\boldsymbol{\rho},k_\perp) = E_0^2\,\exp\left[\frac{1}{2}\left(<\varphi_1^2(\mathbf{r})> + <\varphi_1^{2*}(\mathbf{r}+\boldsymbol{\rho})>\right) + <\varphi_1(\mathbf{r})\,\varphi_1^*(\mathbf{r}+\boldsymbol{\rho})> + 2\,\mathrm{Re}<\varphi_2>\right]\exp(-i\,\rho_y\,k_\perp), \tag{9}$$

where: E_0^2 is the intensity of an incident radiation. In the ray-(optics) approximation describing multiple scattering in the random media, the condition $\sqrt{\lambda L} << l_\varepsilon$ is fulfilled, but it neglects the diffraction effects. If a distance L travelled by the wave in a turbulent magnetized plasma is substantially big, $L >> (l_\varepsilon / \lambda)$, diffraction effects become essential. The smooth perturbation method is a more general method for the solution of diffraction effects if the parameter λ / l_ε is small. SPS of the scattered field in case of an incident plane wave is easily calculated by Fourier transform of the transversal correlation function of a scattered field [1]. If the angular spectrum of an incident wave has a finite width and its maximum is directed along the Z-axis, SPS of the scattered radiation is given by [4, 7, 8]:

$$I(k) = \int_{-\infty}^{\infty} dk_\perp \int_{-\infty}^{\infty} d\rho_y\; W_{EE^*}(\rho_y,k_\perp)\,\exp(i\,k\,\rho_y - k_\perp^2\,\beta^2), \tag{10}$$

where β characterizes the dispersal of an incident radiation (disorder of an incident radiation)

Usually in scintillation studies, the fluctuations are characterized by a scintillation index whose properties can be related to those of the ionospheric irregularities by the application of the diffraction theory. Information about the irregularity electron density spectrum (the so-called "wavenumber spectrum"), the irregularity velocity, and the equivalent thickness of the scattering plasma layer can be deduced using the conventional diffraction theory. To compare the one-dimensional in-situ results, $P_N(k_x)$, with the scintillation results, $P_{SN}(k_x)$, a three-dimensional wavenumber spectrum of electron density irregularities should be integrated [11]:

$$P_{SN}(k_x,L) = 2\pi\,\mathrm{v}_0^2\,k_0^2\,L\int_{-\infty}^{\infty} dk_y\;V_N(k_x,k_y,k_z=0)\;\sin^2\left(\frac{k_x^2+k_y^2}{k_f^2}\right). \tag{11}$$

where $\mathrm{v}_0 = \omega_{p0}^2/\omega^2$. The Fresnel oscillations are smeared by the finite thickness of the irregular layer. This effect can be calculated for a one-dimensional model and weak scattering.

The two-dimensional power spectrum of the phase fluctuations $W_\varphi(k_x,k_y,L)$ and the two-dimensional fluctuating received power $P_S(k_x,k_y,L)$ are related as:

$$P_S(k_x,k_y,L) = 2\,W_\varphi(k_x,k_y,L)\left[1-\left(\frac{k_{fL}}{k_x}\right)^2\sin\left(\frac{k_x}{k_{fL}}\right)^2\cos\left(2\,\frac{k_x^2+k_y^2}{k_f^2}\right)\right], \tag{12}$$

where $k_{fL} = k_0\,(2/k_0\,L)^{1/2}$. The spatial autocorrelation function of the diffraction pattern could be measured with a suitable two-dimensional array of sensors.

For the transition from the three-dimensional function to the one-dimensional one we shall use the assumption of "frozen-in" irregularities, moving without evolution with a velocity V normal to the direction of the wave. We assume that irregularities drift across the beam of the radio signals without changing their shapes. If rigid plasma irregularities are assumed to be moving in the Y direction with apparent velocity V_y transverse to the line of the sight path, the power spectrum $P_S(\nu,L)$, scintillation level S_4 (zeroth moment) and the spectral width (1st moment) which is a measure of the scintillation rate in one-dimensional case are computed from the power spectrum [11]:

$$P_\varphi(\nu, L) = \frac{2\pi}{V_y} \int_0^\infty dk_x \, W_\varphi \left(k_x, k_y = \frac{2\pi\nu}{V_y}, L \right), \quad P_S(\nu, L) = 4\, P_\varphi(\nu, L) \sin^2 \left(\frac{\nu}{\nu_f} \right)^2, \tag{13}$$

$$S_4^2 = \int_0^\infty d\nu \, P_S(\nu, L), \quad \nu_{1S} = \frac{1}{S_4^2} \int_0^\infty d\nu \;\, \nu \, P_S(\nu, L). \tag{14}$$

The Fresnel frequency $\nu_f = V_y / (\pi \lambda z)^{1/2}$ is directly proportional to the drift velocity V_y of plasma irregularities transverse to the radio path and inversely proportional to the Fresnel radius, the slower scintillation frequencies (ν) range $\nu < \nu_f$ is of interest; $(\lambda z)^{1/2}$ is the Fresnel radius, z is the mean height of the randomly inhomogeneous scattering layer or mean distance between the observer and the irregularities. The sinusoidal term in Equations (11)-(13) is responsible for oscillations in the scintillation spectrum. The scintillation level S_4 describing two dimensional diffraction patterns at the ground illustrating the attenuation of the interference pattern can be obtained from Equations (5), (6) (12) and (14).

Information about the irregularity velocity, the thickness of the scattering magnetized plasma layer, and the irregularity electron density spectrum can be deduced calculating statistical characteristics of scattered radio waves taking into account the anisotropy factor, the angle of inclination of prolate irregularities with respect to the external magnetic field, polarization coefficients including fluctuating plasma parameters and the angle between wavevector of scattered radio waves and the external magnetic field.

III. NUMERICAL CALCULATIONS

The incident electromagnetic wave has a frequency of 40 MHz ($k_0 = 0.84\ \text{m}^{-1}$). Plasma parameters at an altitude of 300 km are: $u_0 = 0.0012$, $\text{v}_0 = 0.0133$, $\sigma_N^2 = 10^{-4}$. The Fresnel radius and the Fresnel wavenumber $k_f = (4\pi / \lambda z)^{1/2}$ are equal to 1.5 km and 2.4 km^{-1}, respectively. The oblique sounding method was used for diagnostics of ionospheric irregularities [12]. Experiments were carried out using "Sura" heating facility. Observations show that the artificial ionospheric turbulence occurs in the ionosphere illuminated by high power HF radio waves. There were a lot of irregularities stretching along the geomagnetic field in this region. On the basis of observations of backscattering signals from the artificially disturbed region of the ionosphere it was established that the transversal scale $l_\perp$ of stretched irregularities varies in the range of 100 – 500 m; the magnitudes of the drift velocity were within the limits 65-270 m/s (the typical velocities of ionospheric motions $V_0 \approx I$ 60-100 m/s), a velocity 100 m/s caused by the steady drifting with the horizontal wind of scattering irregularities embedded in the ionosphere will be used in numerical calculations; the spectral index varies in the interval $p = 1.4 \div 4.8$ in different heating sessions. For the case of equatorial scintillation due to field-aligned irregularities with east-west drift motion, χ can be much greater than one. The formation mechanism of small-scale F region irregularities is of an electrodynamic or hydromagnetic nature. The irregularity model is described by a three-dimensional correlation function of the electron density. The surfaces have the form of ellipsoids of revolution with their long axes along the direction of the magnetic field. Numerical calculations are carried out for both Gaussian and power-law spectra for prolate ionospheric irregularities. The spectral density function which best describes the irregularities in a randomly inhomogeneous magnetized plasma depends on the particular case. Most widely used is the spectral density function in the Gaussian, which has certain mathematical advantages. However, power-law spectral densities have been receiving more attention as being physically more realistic. Knowledge of the power spectrum of ionospheric refractive index fluctuations can lead to an understanding of the physical processes that characterize the region of the ionosphere under study.

The anisotropic three-dimensional spectral features are defined for Gaussian spectrum as [5]:

$$V_N(\mathbf{k}) = \sigma_N^2 \, \frac{l_\perp^2 \, l_\parallel}{8\pi^{3/2}} \, \exp\left(-\frac{k_x^2 \, l_\perp^2}{4} - p_1 \frac{k_y^2 \, l_\parallel^2}{4} - p_2 \frac{k_z^2 \, l_\parallel^2}{4} - p_3 \, k_y \, k_z \, l_\parallel^2 \right), \tag{15}$$

where

$$p_1 = (\sin^2\gamma_0 + \chi^2 \cos^2\gamma_0)^{-1} \left[1 + (1 - \chi^2)^2 \sin^2\gamma_0 \cos^2\gamma_0 / \chi^2 \right],$$

$$p_2 = (\sin^2\gamma_0 + \chi^2 \cos^2\gamma_0) / \chi^2, \;\; p_3 = (1 - \chi^2) \sin\gamma_0 \cos\gamma_0 / 2\chi^2,$$

σ_N^2 is the variance of electron density fluctuations. This function contains the parameter $\chi = l_{\parallel} / l_{\perp}$ (ratio of longitudinal and transverse linear scales of plasma irregularities) that measures the anisotropy of the irregularities and the inclination angle γ_0 of prolate irregularities with respect to the external magnetic field.

Measurements of satellite's signal parameters passing through ionospheric layer and measurements aboard of satellite show that irregularities in *F*-region of the ionosphere have power-law spectrum with different spatial scales. A generalized correlation function for power-law spectrum of electron density irregularities with a power-law index *p* has been proposed in [13]. For $p > 3$ the spatial power-law spectrum has the following form:

$$V_N(\mathbf{k}) = \frac{\sigma_N^2}{\pi^{5/2}} \Gamma\left(\frac{p}{2}\right) \Gamma\left(\frac{5-p}{2}\right) \sin\left[\frac{(p-3)\pi}{2}\right] \frac{l_{\parallel}^3}{\chi^2 \left[1 + l_{\perp}^2 (k_{\perp}^2 + \chi^2 k_{\parallel}^2)\right]^{p/2}} , \tag{16}$$

where $\Gamma(x)$ is the gamma function.

Substituting Equation (16) into Equations (6), (11) and (12), the scintillation spectrum of plasma irregularities for power-law spectral function with the index of 4 is illustrated in Figure 1a on a log-log plot. The break point is at $k_x / k_f = 1$. The gap in the normalized power spectrum at $(k_x / k_f) = 1.78$ increases in proportion to the anisotropy factor χ:

$$P_{SN}(k_x, L) = \frac{1}{\sqrt{\pi}} \frac{T k_0 L \mathrm{v}_0^2}{\chi^3} \left\{ \pi \frac{\Gamma\left(\frac{p-1}{2}\right)}{\Gamma\left(\frac{p}{2}\right)} \left(1 + \frac{k_x^2}{k_f^2}\right)^{(1-p)/2} + \chi \int_{-\infty}^{\infty} dz \left(1 + \frac{k_x^2}{k_f^2} + z^2\right)^{-p/2} \cdot \right.$$
$$\left. \cdot \left[-\cos\left(2 \frac{k_x^2}{k_f^2}\right) \cos(2 z^2) + \sin\left(2 \frac{k_x^2}{k_f^2}\right) \sin(2 z^2) \right] \right\} \tag{17}$$

where $T = k_0 l_{II}$. Smearing could be caused by several factors, e.g. a vertical gradient of horizontal drift velocity, the thickness of the scattering medium and/or multiple scattering. The nonstationarity of these parameters could cause smearing. Figure 1b shows the dependence of the SPS of the scattered ordinary wave for the Gaussian spectrum (15) in the direction perpendicular to the principle plane (along the *X*-axis). The longitudinal characteristic linear scale of plasma irregularities $l_{II} = 2$ km, $\chi = 18$, the inclination angle of prolate irregularities with respect to the external magnetic field $\gamma_0 = 10^0$, $\alpha = 20^0$, the distances between the observation points are $\rho_x \approx \rho_y = 500$ m. Numerical calculations show that varying the thickness of a plasma slab from 12 km up to 190 km, the first oscillation minimum ν_1 occurs at: 127 mHz, and the following minimums occur at: $\nu_2 = 230$ mHz, $\nu_3 = 338$ mHz, $\nu_4 = 441$ mHz (Figure 1b).

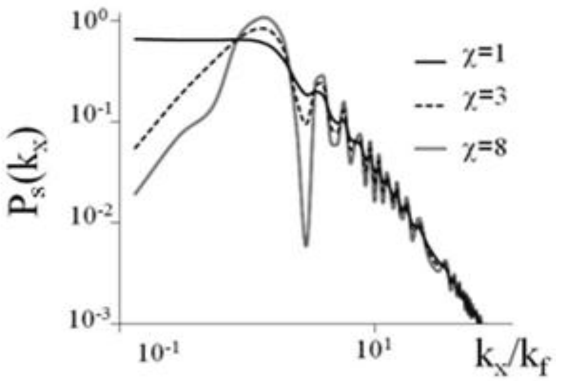

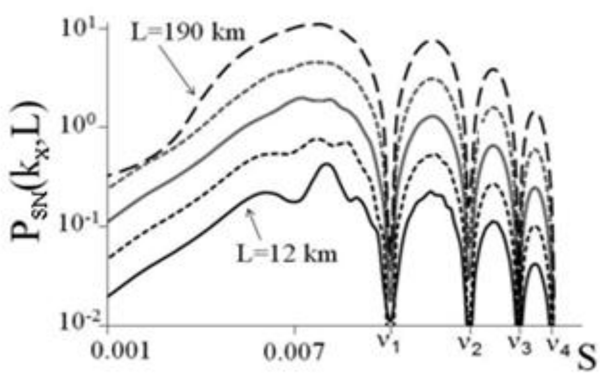

Fig. 1 illustrates the log-log plots of the normalized scintillation spectrum of electron density fluctuations (irregularities) in the *X* direction for power-law spectrum and different anisotropy factor χ (left figure); the SPS of phase fluctuations for the anisotropic Gaussian spectrum versus non-dimensional wavenumber parameter *s* on logarithmic axes and different thickness of a plasma slab (right figure)

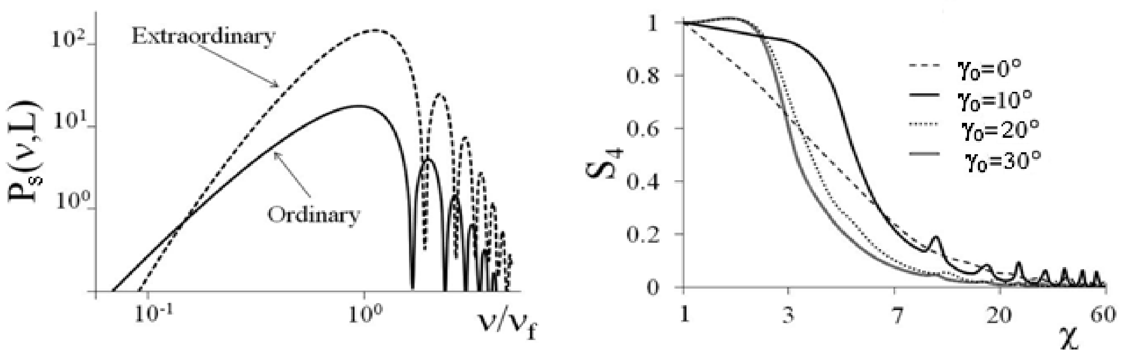

Fig. 2 Depicts the normalized power spectrum of both the ordinary and extraordinary waves as log-log plots versus parameter ν/ν_f at $\chi=5$ and with $T=250$, $\alpha=30^0$, $\gamma_0=10^0$ (left figure); and the scintillation index of scattered ordinary wave as a function of χ for $\alpha=20^0$, $l_{\square}=600$ m, and different angle of inclination $\gamma_0=0^0 \div 30^0$ (right figure)

A phase switch depends on the ratio between the scintillation frequency ν and the Fresnel frequency $\nu_f = V_y/(\pi\lambda z)^{1/2}$. We suppose that the drift velocity transverse to the radio path is equal to $V_y = 100$ m/s, $\alpha=30^0$. Numerical calculations have been carried out for ordinary (*o*-wave) and extraordinary (*e*-wave) waves scattered in the principle plane (5) and anisotropic Gaussian spectrum (15) at $\nu_f = 38$ mHz (Figure 2a). If prolate plasma irregularities with $l_{II}=300$ m, $\chi=5$ are stretched $(\gamma_0=0^0)$ along the external magnetic field, the behavior of the ordinary and extraordinary waves is the same. A maximum of the power spectrum is at 39 mHz, the first minimum is at 68 mHz, the next minimums are at: 95 mHz, 117mHz, 149 mHz. These frequencies satisfy the relations: $1:\sqrt{2}$, $1:\sqrt{3}$, $1:\sqrt{4}$ and so on, which is in a good agreement with the scintillation spectrum when the Fresnel scintillations are observed [2]. Increasing the angle $\gamma_0=10^0$ the power spectrum for the *o*-wave reaches maximum at $\nu_{\max}^{(o)}=36.4$ mHz, for *e*-wave at $\nu_{\max}^{(e)}=45.1$ mHz. The temporal spectrum for *o*-wave has minimums at the frequencies: 68 mHz, 96 mHz, 118 mHz, 136 mHz; for *e*-wave at: 76 mHz, 107 mHz, 131 mHz, 152 mHz. Spectral minimums for the *e*-wave exceed corresponding frequencies for the *o*-wave. The frequency shift of minimums of these waves increases in proportion to the order. Particularly, for the first minimum the frequency shift is equal to 8 mHz, for the fourth minimum is 16 mHz. Varying angle γ_0, the behavior of the scintillation spectrum (maximums and minimums) is different for ordinary and extraordinary waves. The rate of the oscillations is dependent on the irregularity velocity. If these oscillation minima are observed and interpreted as a Fresnel filtering effect, then the Fresnel frequency can be calculated for both ordinary and extraordinary waves. In addition, if the Fresnel frequency can be deduced when the scattering is weak, then the irregularity velocity can be calculated directly. *F*-region scintillations are sensitive to irregularity sizes smaller than the Fresnel radius. The calculations show that the scintillation spectral minimums or Fresnel oscillations are smeared for an irregular layer thickness.

This effect has never been observed experimentally, although both interplanetary and ionospheric scintillations have been observed extensively. The behavior of a temporal spectrum and scintillation level for the *o*-wave and *e*-wave scattered in turbulent magnetized plasma taking into account the movement of plasma irregularities and diffraction effects have been revealed for the first time. The location of these minimums can be used to determine k_f and ν_f. The numerical calculations show that in this case (at $l_{II}=300$ m the variation of the angle γ_0 at the fixed parameter χ has a weak influence on the scintillation index S_4, while at $\gamma_0=0^0$ (the irregularities are considered aligned along the magnetic field) and $\alpha=20^0$ the anisotropy factor χ increases from 5 up to 10, the scintillation level S_4 decreases twice from 0.56 (large scintillation level) to 0.28 (small scintillation level) [11]. Small-level scintillations are also usually associated with both positive and negative intensity fluctuations about the mean level. Hence, the influence of anisotropy of plasma irregularities on S_4 is stronger than the inclination angle of prolate irregularities with respect to the external magnetic field.

Substituting (16) into (5) and (14), the scintillation level in the principle plane has the following form:

$$S_4^2 = \frac{8\,\tilde{\Omega}_5 Q}{\pi}\int_{-\infty}^{\infty} ds \int_{-\infty}^{\infty} dx\ \frac{x^2 + \mathrm{P}_j^2\,(\mu+s)^2}{(\delta_4 + x^2)^2}\ \frac{\sin^2\left[k_0 L\,(x^2+s^2)\right]}{\left\{1+T^2\left[\dfrac{x^2+s^2}{\chi^2}+\dfrac{(\delta_2\,x^2+\delta_3)^2}{(\delta_4+x^2)^2}\right]\right\}^{p/2}}. \qquad (18)$$

where

$$Q = \Gamma\left(\frac{p}{2}\right)\Gamma\left(\frac{5-p}{2}\right)\sin\left[\frac{(p-3)\,\pi}{2}\right],$$

$$\delta_3 = \mathrm{P}_j\, s\left[\mathrm{P}_j\,\mu - 2\Gamma_j\,\mu^2 + (\mathrm{P}_j - 3\Gamma_j\,\mu)\, s - \Gamma_j\, s^2\right],$$

$$\delta_2 = 1 - \mathrm{P}_j\,\Gamma_j\,(\mu + s),\ \delta_4 = \mathrm{P}_j^2\,(\mu+s)^2 .$$

The analysis shows that an ordinary radio wave scattered on irregularities $l_{II} = 2$ km of electron density fluctuations has a large scintillation level $S_4 = 0.6$ for both power-law spectrum with $p = 4$, $\alpha = 0^0$, $\chi = 2$ and Gaussian spectrum at $\gamma_0 = 0^0$. A small scintillation level $S_4 = 0.2$ appears for these spectra at $\chi = 3$ and $\chi = 4$, respectively. Numerical calculations also show that for the power-law spectrum with $p = 4$, $\alpha = 20^0$ and $\chi = 1$ the scintillation index is equal to $S_4 = 0.82$ (for the *o*-wave) and $S_4 = 0.23$ (for the *e*-wave); by increasing the anisotropy factor up to $\chi = 22$, the scintillation index tends to saturation $S_4 = 0.55$ (large scintillation level) for the *o*-wave and $S_4 = 0.16$ (small scintillation level) for the *e*-wave. Small-level scintillations are usually associated with a fast scintillation rate (large ν_{1S}). Furthermore, small-level scintillations are also associated with both positive and negative intensity fluctuations about the mean level, while the large level tends to correspond to the slower scintillation level with primarily positive intensity fluctuations.

Figure 2b represents log-log plots of the scintillation level for the anisotropic Gaussian spectrum versus anisotropy factor χ at fixed parameters $\alpha = 20^0$, $l_{\|} \approx 1$ km and different angle of inclination γ_0. In this case the parameter S_4 oscillates with $\gamma_0 = 10^0$. The first maximum $S_4 = 0.41$ is at $\chi = 11$, the second maximum $S_4 = 0.18$ at $\chi = 18$, the third one $S_4 = 0.2$ at $\chi = 24$. Hence the scintillation level varies within $0.2 \div 0.4$. The first moment of the power spectrum (14) describing the spectral width is in the interval 20 mHz $\leq \nu_{1S} \leq$ 23 mHz. These data are in agreement with the results obtained in [14].

Substituting (15) into (6) and (14), we calculate the normalized scintillation level for the *o*-wave and *e*-wave scattered in magnetized plasma in the direction perpendicular to the principle plane (along the *X*-direction):

$$\frac{S_4}{\sqrt{2<\varphi_1^2>}} = \left\{8\int_{-\infty}^{\infty} ds\ \frac{1}{\sqrt{b_3}}\ \sin^2\left[\left(\frac{k_0}{k_f}\right)^2 s^2\right]\exp\left(-\frac{T^2}{4}\,b_4\right)\right\}^{1/2}\left[\int_{-\infty}^{\infty} ds\ \frac{1}{\sqrt{b_1}}\ \exp\left(-\frac{T^2}{4}\,b_2\right)\right]^{-1/2}, \tag{19}$$

where

$$b_1 = \frac{1}{4\chi^2} - \frac{1}{64}\,p_2\left[2(\Gamma_j + \mathrm{P}_j\,\mu) - \Gamma_j\, s^2\right]^2 + \frac{1}{4}\,\mathrm{P}_j\,\Gamma_j\left(\frac{1}{2}\,p_2\,\mu + p_3\right)s,\ \ b_2 = \frac{1}{4}\,(p_1 + p_2\,\mu^2 + 4p_3\,\mu)\, s^2,$$

$$b_3 = g_1\, s^3 + g_2\, s^2 + g_3\, s + \frac{1}{\chi^2},\ \ b_4 = \frac{1}{4}\,p_2\, s^4 + (p_2\,\mu + 2\,p_3)\, s^3 + (p_1 + p_2\,\mu^2 + 4\,p_3\,\mu)\, s^2,\ \ g_1 = \frac{1}{4}\,p_2\,\mathrm{P}_j\,\Gamma_j\ ,$$

$$g_2 = p_2\left(\frac{1}{2}\mathrm{P}_j\,\Gamma_j\,\mu + a_0\right) + p_3\,\mathrm{P}_j\,\Gamma_j,\ \ g_3 = 2\,(p_2\, a_0\,\mu + 2\,p_3\, a_0),\ \ a_0 = \frac{1}{4}\,(\mu\,\mathrm{P}_j + \Gamma_j)\,\Gamma_j .$$

The normalized scintillation level $S_4/\sqrt{2<\varphi_1^2>}$, including small and large scintillation levels, for scattered radio waves in magnetized plasma, is presented in Figure 3a. Numerical calculations were carried out for the following parameters: $l_{\|} = 120$ m, $\alpha = 20^0$ and $\gamma_0 = 10^0$. In the isotropic case ($\chi = 1$), significant filtering (oscillations) appears at $(k_0/k_f) = 68$ corresponding to the distance of 11 km from the irregular plasma layer. Increasing the anisotropy factor up to 15, scintillation level oscillates at a distance of 1 km from a slab, $(k_0/k_f) = 20.6$. Oscillations of the scintillation level from a plasma layer boundary started in proportion to the anisotropy factor of prolate irregularities. For electron density irregularities with $l_{II} = 180m$, significant filtering appears, that is, the normalized scintillation level oscillates at the distances of 4.5 km and 4.3 km from a plasma layer for the *o*-wave and *e*-wave, respectively (Figure 3b). To properly interpret different features in the observed power spectra, one must estimate within what limits the observed spectrum approximates the true spectrum. Also the frequency resolution or resolution bandwidth must be less than the expected spectral oscillations.

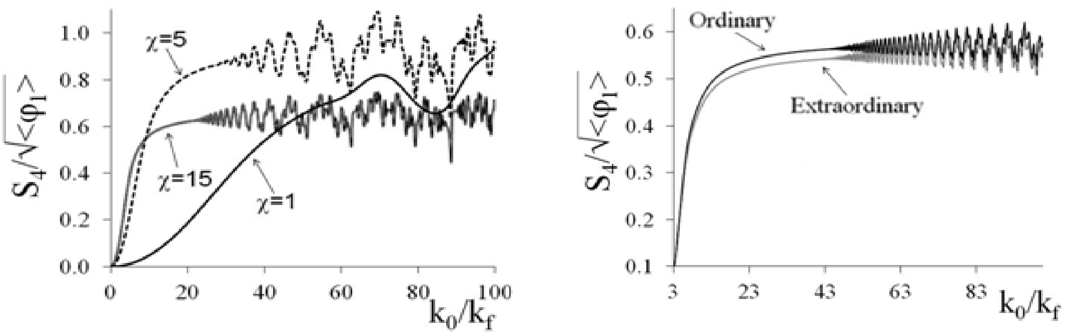

Fig. 3 Normalized scintillation level as a function of distance below an irregular plasma layer based on anisotropic Gaussian irregularities in the direction perpendicular to the principle plane, χ is effective axial ratio in a plane normal to the radio path

One of the most important second order statistical characteristics is a wave structure function. Plots of the phase wave structure function D_S of the scattered ordinary wave in the principal plane for the anisotropic Gaussian spectrum as a function of η with $\gamma_0 = 0^0 \div 15^0$ are presented in Figure 4a. Numerical calculations show that maxima of the D_S function are at $\eta = 31$ with $\gamma_0 = 0^0$; and at $\eta = 59$ with $\gamma_0 = 5^0$; the phase wave structure function tends to saturation at $\eta = 450$. Analyses show that the angle-of-arrival in the principle plane is in the interval of $0.5'' \div 2'$. Figure 4b depicts the dependence of the three-dimensional wave structure function $D_{\chi S}$ of the mutual correlation function of the amplitude and phase fluctuations for the extraordinary wave versus distances between the observation points locating in perpendicular directions for the power-law

spatial spectrum (16). If $p = 4$, $\alpha = 20^0$, $k_\perp = 0.114$, $l_{\square} = 100$ m, $\chi = 3$, numerical calculations show that $D_{\chi S}$ for the *e*-wave substantially exceeds similar correlation for the *o*-wave. Oscillations of this wave structure function increases inversely proportional to the longitudinal characteristic linear scale of electron density fluctuations and hence diffraction effects appear more vividly. The finite diameter of the radio sources could possibly affect the scintillation rate. Simultaneous satellite and stellar measurements at times of large scintillation levels would help to better understand these scale changes.

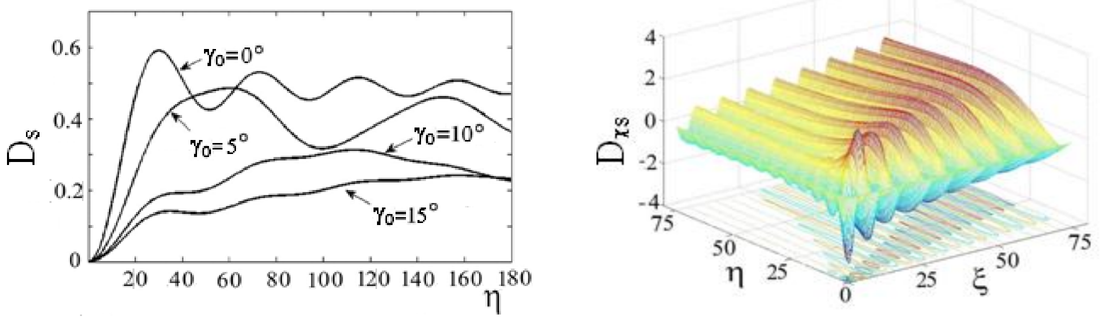

Fig. 4 Phase wave structure function as a function of the distance between observation points η in the principle plane at, $\chi = 10$, $\alpha = 20^0$ for $P_S(\nu, L)$ (left figure). Three-dimensional wave structure function $D_{\chi S}$ of the correlation functions of amplitude and phase fluctuations versus distances between observation points for the *e*-wave at $T = 80$, $\chi = 3$ (right figure)

Substituting Equation (16) into Equations (6), (9) and (10), the SPS of power-law correlation functions of electron density fluctuations in turbulent non-magnetized plasma has the form:

$$\frac{W_{EE^*}(\xi,\eta,L)}{E_0^2} = \exp(-i\eta\mu)\cdot\exp\left(\pi^{3/2}\frac{T^2\, \mathrm{v}_0^2\, Q_0}{\chi\,\Gamma\left(\frac{p}{2}\right)}\, k_0\, L\, \left\{-\frac{1}{2}\,\Gamma\left(\frac{p-1}{2}\right)\int_{-\infty}^{\infty} ds\, \frac{1}{(1+C_1 s^2)^{p-1}} + \left(\frac{\chi\,\xi}{2\,T}\right)^{(p-1)/2} \cdot \right.\right. \tag{20}$$

$$\left.\left. \cdot\int_{-\infty}^{\infty} ds\, \frac{\exp(-i\eta s)}{\left[1+\Phi(s)\right]^{(p-1)/2}}\;\; K_{\frac{p-1}{2}}\left(\frac{\chi\,\xi}{T}\left[1+\Phi(s)\right]\right)\right\}\right)$$

where: $Q_0 = \dfrac{\sigma_N^2}{\pi^{5/2}}\,\tilde{Q}$, $\Phi(s) = \dfrac{T^2}{4}\left[s^4 + 4\mu s^3 + 4\left(\dfrac{1}{\chi^2} + \mu^2\right)s^2\right]$, $C_1 = \dfrac{T^2}{\chi^2}(1+\chi^2\mu^2)$, $K_\nu(x)$ is the McDonald function.

Figure 5a illustrates the "Double-humped effect" of the scattered *o*-wave in turbulent anisotropic collisionless non-magnetized plasma with prolate irregularities of electron density fluctuations having characteristic longitudinal linear scale $l_{\parallel} = 10$ km; the spectral index is equal to $p = 3.2$. Numerical calculations show that the electromagnetic wave with parameters $\mu = 0.05$, $\alpha = 20^0$, $\beta = 10$ travelling at a distance of 2000 km in the ionosphere broadens on 56% increasing anisotropy factor of prolate irregularities from $\chi = 150$ up to 350. Figure 5b represents the evaluation of a gap in the SPS of the scattered ordinary wave in magnetized plasma versus the wavenumber *k* in the direction perpendicular to the principle plane for the power-law spectrum with $\mu = 0.05$, $\alpha = 20^0$, $\beta = 10$, $l_{\parallel} = 10$ km, $\chi = 350$, the power-law index $p = 3.2$ and the different value of the parameter B_0. The numerical analyses show that the depth of a gap in the SPS increases by 61% when a radio wave in turbulent plasma travels 2300 km.

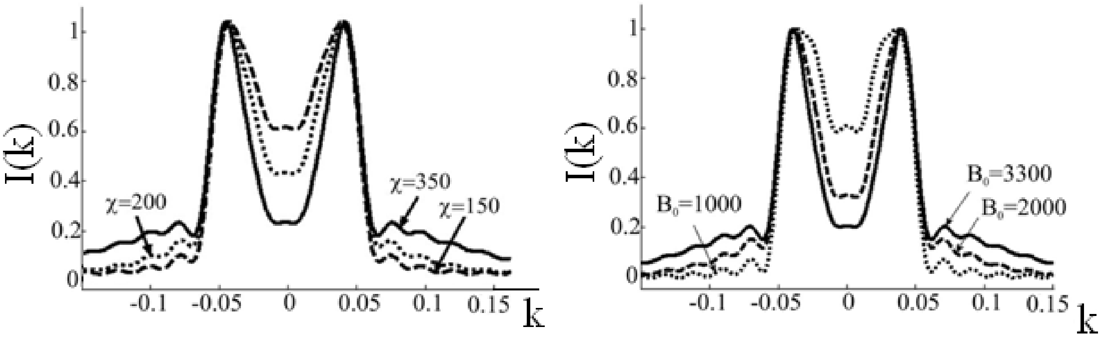

Fig. 5 Depicts SPS of scattered *o*-wave versus *k* for $\mu = 0.05$, $\alpha = 20^0$, $\beta = 10$, at fixed $B_0 = 3300$, plasma parameters: $p = 3.2$, $l_{\parallel} = 10$ km, $L = 1000$ and different anisotropy factor $\chi = 150$, 200, 350 (left figure); the SPS of scattered *o*-wave as a function of k for $\alpha = 20^0$, $p = 3.2$, $l_{\parallel} = 10$ km, B_0 = 1000, 2000, 3300 (right figure)

IV. CONCLUSIONS

Second order statistical moments of scattered ordinary and extraordinary electromagnetic waves in turbulent anisotropic magnetized plasma: the correlation function of the phase fluctuation and the scintillation level are obtained for the arbitrary correlation function of electron density fluctuations. The velocity of rigid plasma inhomogeneities, the equivalent thickness of the scattering layer, the irregularity electron density spectra, anisotropy factor and the angle of inclination of prolate irregularities with respect to the external magnetic field, polarization coefficients including fluctuating plasma parameters and the angle between the scattered radio waves and the external magnetic field are taken into account when calculating statistical characteristics of scattered radio waves in magnetized plasma. Numerical calculations were carried out for both anisotropic Gaussian and power-law correlation functions.

New peculiarities of the "Double-humped effect" in the SPS of the multiple scattered electromagnetic waves at oblique illumination of magnetized plasma with prolate irregularities by mono-directed incident radiation have been revealed for the first time for the power-law spectrum of electron density fluctuations, using the smooth perturbation method and taking into account diffraction effects. It was established that the SPS has a double-peaked shape, the location of its maximum weakly varies and width substantially broadens increasing distance travelling by radio waves in turbulent anisotropic magnetized plasma. The anisotropy factor and the angle of inclination of prolate irregularities have a substantial influence on a gap of the SPS.

The dependence of the scintillation spectrum on the anisotropy parameters of prolate plasma irregularities for the ordinary and extraordinary waves in turbulent magnetized plasma taking into account movement of plasma irregularities and diffraction effects has been revealed for the first time. Maximums and minimums of this spectrum have been established for the drift velocity $V_y = 100$ m/s. If anisotropic irregularities of electron density fluctuations are stretched along the external magnetic field, the behavior of the ordinary and extraordinary waves is the same: Frequencies of the Fresnel scintillation spectrum minimums satisfy the relations: $1:\sqrt{2}$, $1:\sqrt{3}$, $1:\sqrt{4}$ and so on. Varying the angle of inclination of prolate irregularities with respect to the external magnetic field, the behavior of the scintillation spectrum (maximums and minimums) is different for both waves. Spectral minimums for the *e*-wave exceed corresponding frequencies for the *o*-wave. If the Fresnel frequency is known, the velocity of the irregularities can be calculated. The power spectral analysis of scintillation observations offers a new and important method of analyzing the small-scale structure in the ionosphere. Large and small scintillation levels for S_4 have been calculated for irregularities aligned along the geomagnetic field of lines. It was shown that the influence of anisotropy of plasma irregularities on S_4 is stronger than the inclination angle of prolate irregularities with respect to the external magnetic field. Oscillations of the normalized scintillation level from a plasma layer boundary started in proportion to the anisotropy factor of prolate irregularities; for the *e*-wave it occurs earlier than for the *o*-wave.

The phase wave structure functions of scattered ordinary wave have been calculated for the anisotropic Gaussian spectrum as a function of distance between observation points spaced apart in the principle and perpendicular planes allowing to calculate the angle-of-arrival of scattered radiation. It is in the interval of $0.5'' \div 2'$.

It is noted that the spectrum of geomagnetic micropulsations is in substantial agreement with the scintillation power spectrum. The geophysicists also interested in both the spectral shape and global morphology of the *F*-region irregularities in hope to get a deeper insight into physical processes which produce them, whereas the radio communicator needs a realistic description of the irregularities on a worldwide basis to model the scintillation behavior for application to existing and future satellite systems. The studies of the scintillation, or the temporal and spatial variations, of amplitude and phase of such a signal have yielded much information about the nature of the responsible ionospheric irregularities. This theory should be useful in developing a worldwide spectral model for *F*-region irregularities. Furthermore, this theory may also be useful in predicting scintillation levels and other effects on transionospheric radio signals.

REFERENCES

[1] Z B. N. Gershman, L. M. Eruxhimov and Yu.Ya. Yashin, *Wavy Phenomena in the Ionosphere and Cosmic Plasma*, Moscow, Nauka, 1984 (in Russian).

[2] A. Ishimaru, A. *Wave Propagation and Scattering in Random Media, Vol. 2, Multiple Scattering, Turbulence, Rough Surfaces and Remote Sensing*, IEEE Press, Piscataway, New Jersey, USA, 1997.

[3] S. M. Rytov, Yu. A. Kravtsov and V. I. Tatarskii, *Principles of Statistical Radiophysics. vol.4. Waves Propagation Through Random Media*. Berlin, New York, Springer, 1989.

[4] V. G. Gavrilenko, G. V. Jandieri, A. V. Sarokin and V. G. Jandieri, “Some properties of the angular power distribution of electromagnetic waves multiply scattered in a collisional magnetized turbulent plasma,” *Plasma Physics Report*, vol. 31, pp. 604-615, 2005.

[5] G. V. Jandieri G.V, A. Ishimaru, V. G. Jandieri, A. G. Khantadze and Zh. M. Diasamidze, “Model computations of angular power spectra for anisotropic absorptive turbulent magnetized plasma,” *Progress In Electromagnetics Research*, vol. 70, pp. 307-328, 2007.

[6] V. G. Gavrilenko, G. V. Jandieri, A. Ishimaru and V. G. Jandieri, “Peculiarities of spatial spectrum of scattered electromagnetic waves in anisotropic inhomogeneous medium,” *Progress In Electromagnetics Research B*, vol. 7, pp. 191-208, 2008.

[7] V. G. Gavrilenko, A. V. Aistov, and G. V. Jandieri, “Some peculiarities of wave multiple scattering in a statistically anisotropic medium,” *Waves Random Media*, vol. 10, pp. 435-445, 2000.

[8] G. V. Jandieri, A. Ishimaru, N. F. Mchedlishvili and I. G. Takidze, “Spatial power spectrum of multiple scattered ordinary and extraordinary waves in magnetized plasma with electron density fluctuations,” *Progress In Electromagnetics Research M*, vol. 25, 87-100, 2012.

[9] G. V. Jandieri and A. Ishimaru, “Some peculiarities of the spatial power spectrum of scattered electromagnetic waves in randomly inhomogeneous magnetized plasma with electron density and external magnetic field fluctuations,” *Progress In Electromagnetics Research B*, vol. 50, pp. 77-95, 2013.

[10] V. L. Ginzburg, *Propagation of Electromagnetic Waves in Plasma*. New York: Gordon and Beach, 1961.

[11] C. L. Rufenach, “Power-law wavenumber spectrum deduced from ionospheric scintillation observations,” *Journal of Geophysical Research*, vol. 77, iss. 25, pp. 4761-4772, 1972.

[12] N. V. Bakhmet’eva, V. N. Bubukina, Yu. A. Ignat’ev, G. S. Bochkarev, V. A. Eremenko, V. V. Kol’sov, I. V. Krasheninnikov and Yu. N. Cherkashin, “Investigation by backscatter radar irregularities produced in ionospheric plasma heating experiments,” *Journal of Atmospheric and Terrestrial Physics*, vol. 59, iss. 18, pp. 2257-2263, 1997.

[13] I. P. Shkarofsky, “Generalized turbulence space–correlation and wave–number spectrum–function pairs,” *Canadian Journal of Physics*, vol. 46, pp. 2133-2153, 1968.

[14] C. L. Rufenach, “Power spectra of large scintillation signals,” *J. of Atmospheric and Terrestrial Physics*, vol. 37, pp. 569-572, 1975.